Electronic Supplementary Information (ESI)

Efficient charge separation and photooxidation on cobalt phosphate-loaded TiO_2 mesocrystal superstructures

Takashi Tachikawa,[a,b] Peng Zhang,[a] Zhenfeng Bian,[a] and Tetsuro Majima*[a]*

[a] The Institute of Scientific and Industrial Research (SANKEN), Osaka University, Mihogaoka 8-1, Ibaraki, Osaka 567-0047, Japan

[b] PRESTO, Japan Science and Technology Agency (JST), 4-1-8 Honcho Kawaguchi, Saitama 332-0012, Japan

tachi45@sanken.osaka-u.ac.jp (T.T.); majima@sanken.osaka-u.ac.jp (T.M.)

S1. Experimental Methods

Materials. The chemicals for synthesis of catalysts were purchased from Aldrich, Wako, and Nacalai Tesque and used without further purification. Commercial ST21 (Ishihara Sangyo) and P25 (Nippon Aerosil) were used as received. MesoTiO_2 and NanoTiO_2 (annealed under oxygen atmosphere at 500°C) were synthesized according to literature procedures.[S1] 3'-*p*-Aminophenyl fluorescein (APF) and 3'-*p*-hydroxyphenyl fluorescein (HPF) were purchased from Sekisui Medical and used without further purification. Fluorescein sodium salt was purchased from Tokyo Chemical Industry and used without further purification. *p*-Benzoquinone was purchased from Aldrich and purified by sublimation before use.

Synthesis of CoPi-TiO_2. In a typical synthesis of CoPi-TiO_2, 3 mg TiO_2 was mixed with a 3 ml solution of 0.5 mM $CoCl_2$ in 0.1 M sodium phosphate (NaPi) buffer at pH 7.0 forming a homogenous suspension. The suspensions were then exposed to UV light (315–400 nm, 580 mW cm^{-2}) from a mercury light source (Asahi Spectra, REX-250) at room temperature. Finally, the suspensions were centrifuged at 10000 rpm (Hitachi, himac CF16RX) to separate the solid products. The products were subsequently washed with Milli-Q water. The amounts of loaded Co were determined by UV-Vis absorption and EDX measurements.

Synthesis of Pt nanoparticle-deposited MesoTiO_2. Pt-MesoTiO_2 was prepared by the photochemical deposition method.[S2] In a typical synthesis, 0.25 g MesoTiO_2, 225 mL of Milli-Q ultrapure water, 25 mL methanol, and H_2PtCl_6 (Aldrich) were mixed forming a homogeneous suspension. The solutions were then exposed to UV light for 30 min at room temperature. Finally, the solutions were centrifuged at 10000 rpm to separate the solid products. The amounts of loaded Pt were determined by inductively coupled plasma (ICP) emission spectroscopy (Shimadzu, ICPS-8100).

Instruments. The samples were characterized using FESEM equipped with EDX analyzer (JEOL JSM-6330FT) and TEM equipped with EDX analyzer (Hitach H-800; operated at 200 kV). The steady-state UV-Vis absorption and diffuse reflectance spectra were measured by UV-Vis-NIR spectrophotometers (Shimadzu, UV-3100, and Jasco, V-570, respectively) at room temperature. The steady-state fluorescence spectra were measured using a HORIBA FluoroMax-4 fluorescence spectrophotometer at room temperature. EPR spectra were recorded on a JEOL JES-RE2X electron spin resonance spectrometer at 77 K. The g values were calibrated using Mn^{2+} in MgO as standard.

Time-Resolved Diffuse Reflectance Measurements. The sample suspensions containing the TiO_2 powders (20 g L^{-1}) were sonicated for 15 min and are placed in 1-mm light path quartz cuvettes before the measurements. The time-resolved diffuse reflectance measurements were performed using the third

harmonic generation (355 nm, 5 ns full width at half-maximum, 1.5 mJ pulse^{-1}, 1 Hz) from a Q-switched Nd^{3+}:YAG laser (Continuum, Surelite II-10) for the excitation operated by temporal control using a delay generator (Stanford Research Systems, DG535). The reflected analyzing light from a continuous wave 450 W Xe-arc lamp (Ushio, UXL-451-0) was collected by a focusing lens and directed through a grating monochromator (Nikon, G250) to a silicon avalanche photodiode detector (Hamamatsu Photonics, S5343). The transient signals were amplified with a voltage amplifier (Femto, DHPVA-100) and recorded by a digitizer (Tektronix, DPO3054). Time profiles were obtained from the average of 8 or 32 laser shots. All experiments were carried out at room temperature. The % absorption (%Abs) is given by equation: $\%Abs = (R_0 - R)/R_0 \times 100$, where R and R_0 represent the intensities of the diffuse reflected monitor light with and without excitation, respectively.

Photooxidation Activity Tests. For typical runs, 3 mL of a phosphate buffer suspension containing TiO_2 (0.07 g L^{-1}), APF (2 μM), and DMSO (100 mM) as an $^{\bullet}OH$ scavenger was sonicated for 20 min, and then transferred into a quartz cuvette. The photochemical reaction was initiated upon irradiation with a mercury light source (Asahi Spectra, REX-250) through a filter (centered at 365 nm) at room temperature. The intensity of the UV light was measured to be 6 mW cm^{-2}. After stopping the UV light illumination, the sample was centrifuged at 10000 rpm (Hitachi, himac CF16RX) to separate the solid particles. The oxidation of APF was monitored by a UV-Vis spectrophotometer and the fluorescence from the products was analyzed by a fluorescence spectrophotometer.

Sample Preparation for Fluorescence Imaging. The cover glasses were purchased from Matsunami glass (Japan) and cleaned by sonication in a detergent solution for 4 h, followed by repeated washings with warm flowing water for 30 min. Finally, the cover glasses were washed again with Milli-Q ultrapure water (Millipore). Well-dispersed buffer suspensions of TiO_2 were subsequently spin-coated on the cleaned cover glasses. The cover glasses were placed in a sample chamber. A TiO_2-coated cover glass was mounted on the bottom of a holder designed for viewing specimens on the microscope. A silicon spacer with a 9 mm pore (Invitrogen) was placed on the TiO_2-coated glass to form a chamber. The chamber was filled with a sample solution and was then covered with a clean cover glass to prevent the solution from escaping.

Single-Particle Fluorescence Measurements with Wide-Field Microscopy. The experimental setup included an Olympus IX81 inverted fluorescence microscope. 488-nm CW laser (Coherent; ~3 W cm^{-2} at the glass surface) and 365-nm LED (Opto-Line; ~5 mW cm^{-2} at the glass surface) sources were used to excite the dyes and TiO_2, respectively. The optical transmission and emission images were recorded on an EMCCD camera (Roper Scientific, Evolve 512) at a frame rate of 20 frames s^{-1} using MetaMorph

(Molecular Devices). All experimental data were obtained at room temperature. Fluorescence images were analyzed using the ImageJ software (http://rsb.info.nih.gov/ij/).

Single-Particle PL Measurements with Time-Resolved Confocal Mcroscopy. Fluorescence lifetime images were recorded using an objective-scanning confocal microscope system (PicoQuant) coupled with an Olympus IX71 inverted fluorescence microscope. The samples were excited through an oil objective (Olympus, UPLSAPO 100XO; 1.40 NA, 100×) with a circular-polarized 485 nm pulsed laser (PicoQuant) controlled by a PDL-800B driver (PicoQuant). An instrument response function (IRF) of ~110 ps was obtained by measuring the scattered laser light in order to analyze the temporal profile. The emission was collected with the same objective and detected by a single photon avalanche photodiode (Micro Photon Devices, PDM 50CT) through a dichroic beam splitter (Chroma, z405/488rpc), a long-pass filter (Chroma, HQ510LP), a band-pass filter (Semrock, FF01-531/40), and a 75-μm pinhole for spatial filtering to reject out-of-focus signals. The data collected using the PicoHarp 300 TCSPC module (PicoQuant) were stored in the time-tagged time-resolved mode (TTTR), recording every detected photon with its individual timing, which were used for the analysis. All the experimental data were obtained at room temperature.

S2. Structural Analysis of Pt-MesoTiO$_2$ and CoPi-Pt-MesoTiO$_2$

Fig. S1 shows the TEM images of Pt nanoparticle-loaded MesoTiO$_2$ (Pt-MesoTiO$_2$). A number of Pt nanoparticles of ~3 nm were deposited on the edge of the well-ordered parts of MesoTiO$_2$ (Fig. S1B,D). Meanwhile, for the broken parts of MesoTiO$_2$, Pt nanoparticles were mostly deposited on the side walls with the anatase{101} facets inside the pores of MesoTiO$_2$ (Fig. S1B,E).

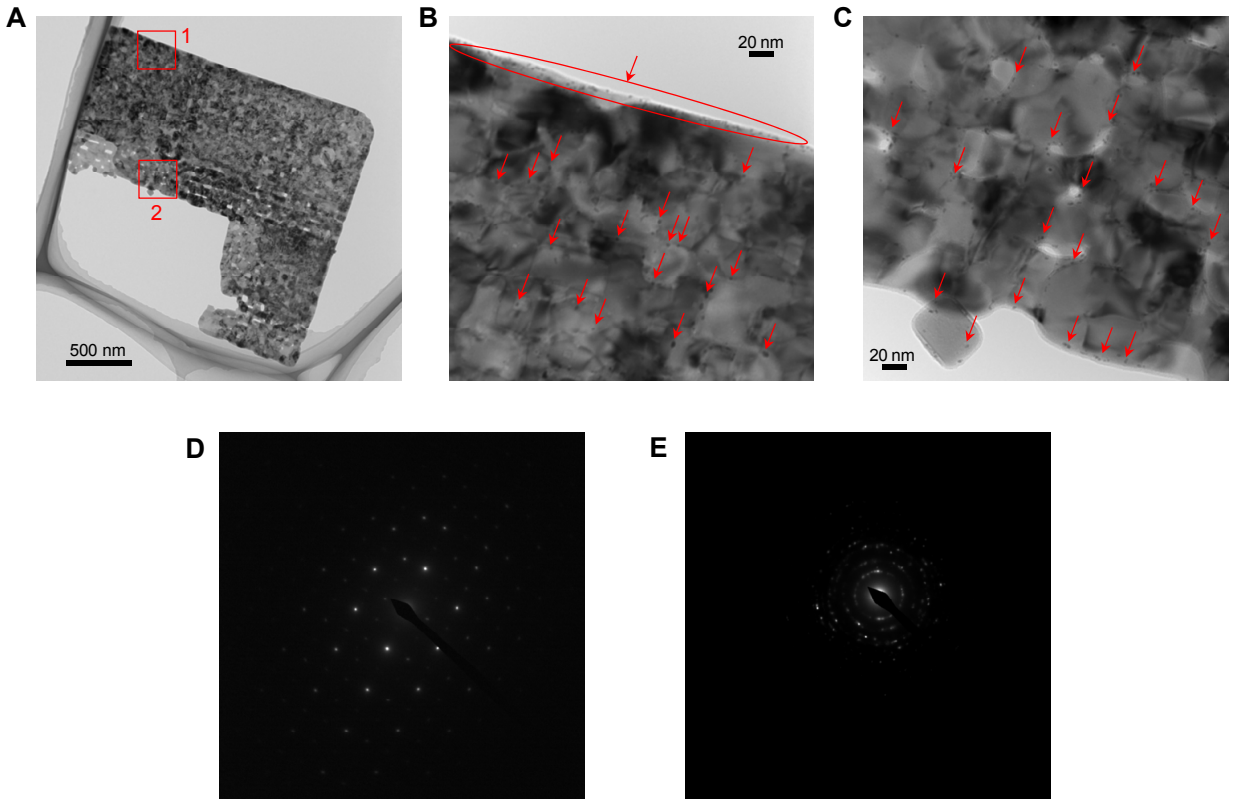

Fig. S1. (A–C) TEM images of Pt-MesoTiO$_2$. The panels B and C represent the enlarged red squares (regions 1 and 2, respectively) in the panel A. The red arrows indicate the locations of Pt nanoparticles. (D,E) Typical selected area electron diffraction patterns of the well-ordered part (D) and the disordered part (*i.e.*, randomly-oriented nanoparticles) (E).

Fig. S2 shows typical TEM images of CoPi and Pt nanoparticle-loaded MesoTiO$_2$ (CoPi-Pt-MesoTiO$_2$-3, see the main text). From the STEM-EDX analysis, the mean Co concentration was determined to be 7.8 ± 2.0 wt% (Fig. S2C).

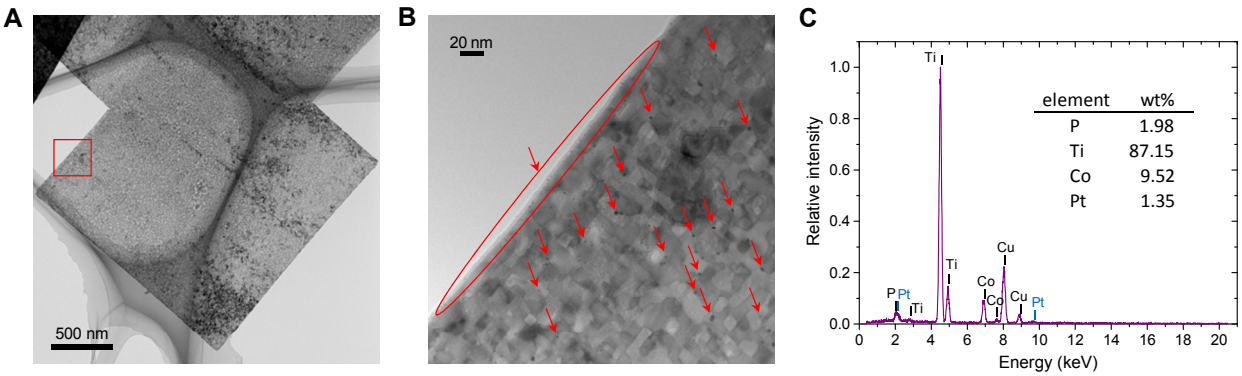

Fig. S2. (A,B) TEM images and (C) EDX spectrum of CoPi-Pt-MesoTiO$_2$-3. The panel B represents the enlarged red square in the panel A. The red arrows indicate the locations of Pt nanoparticles.

S3. Mechanism of Oxidation of APF and HPF

APF and HPF were originally designed as specific fluorescence probes for $^{\bullet}$OH by Nagano and co-workers.[S3] As demonstrated in the main text, fluorescence intensity increased significantly upon UV light irradiation of the suspension containing TiO$_2$, APF (or HPF), and DMSO as an $^{\bullet}$OH scavenger. Since DMSO concentration (100 mM) is about three orders of magnitude higher than the concentration of probe dyes (2 μM), the involvement of $^{\bullet}$OH in the oxidation of the probe dyes should be excluded. To clarify the oxidation mechanism, we analyzed the products with a Thermo Scientific LTQ Orbitrap XL hybrid Fourier-transform mass spectrometer (MS). The mass numbers of the identified products are summarized in Table S1. Fluorescein was detected as a main product and *p*-benzoquinone imine and *p*-benzoquinone (as semiquinone radical anion) were detected as byproducts for APF and HPF, respectively. The MS peaks assigned to the dimerization products and OH-adducts of APF and HPF were not observed. Furthermore, as shown in Fig. S3, fluorescence lifetime measurements revealed that the lifetime of the products is in agreement with that of fluorescein, thus supporting the generation of fluorescein from APF during TiO$_2$-assisted photochemical reactions.

A possible mechanism for TiO$_2$-assisted oxidation of APF and HPF is proposed in Scheme S1. Both TiO$_2$ holes and active Co$^{III/IV}$ species in CoPi oxidize the *p*-aminophenyl group of APF (*p*-hydroxyphenyl group of HPF) to induce *O*-dearylation reaction. Similar mechanism has been proposed

for oxidative *O*-dealkylation reactions of alkyl aryl ethers mediated by several chemical and biological oxidizing systems.[S5,S6]

Table S1. MS Characterizations of Substrates and Products

sample	mass number	
	obs. [b]	calc.
products (Pt-P25/APF/DMSO) [a]	107.0378 331.0615 (422.1037)	–
products (Pt-P25/HPF/DMSO) [a]	108.0219 331.0617 (423.0882)	–
APF	422.1039	423.11
HPF	423.0880	424.10
fluorescein	331.0618	331.06
p-benzoquinone imine	–	107.04
p-benzoquinone	108.0219 [c]	108.02

[a] [Pt-P25] = 0.75 g L^{-1}, [APF(HPF)] = 10 μM, [DMSO] = 100 mM in pH 10 water (NaOH). UV light irradiation time was 3 min. The products were purified by (deactivated) alumina chromatography.
[b] Detected by APCI with negative ion mode
[c] Detected as semiquinone radical anion ($C_6H_4O_2^{\bullet-}$) (mass number = 108.02) that results from collision induced loss of H from the hydride adduct.[S4]

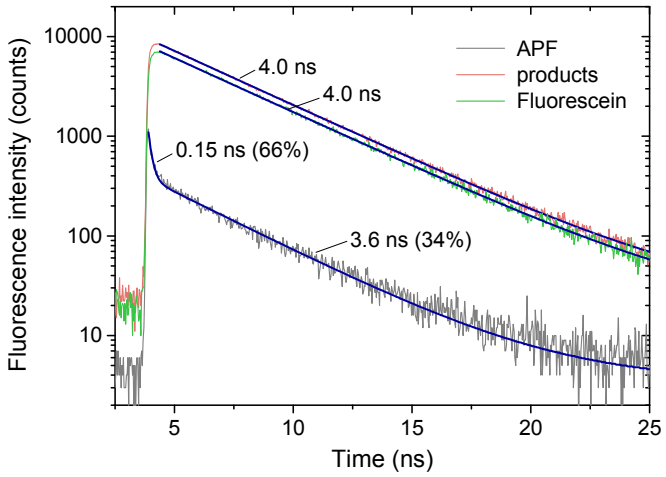

Fig. S3. Fluorescence decay profiles of APF (2 μM), reaction products, and fluorescein (200 nM) in phosphate buffer solutions (0.1 M, pH 7.0). The reaction products were obtained by UV light irradiation (6 min) of the buffer suspension of CoPi-MesoTiO_2 (0.07 g L^{-1}) and APF (2 μM). The catalyst was removed by centrifugation for measurements. The blue lines are exponential curves fitted to the kinetic traces.

Scheme S1. TiO_2-Assisted Oxidation Processes of APF and HPF on TiO_2

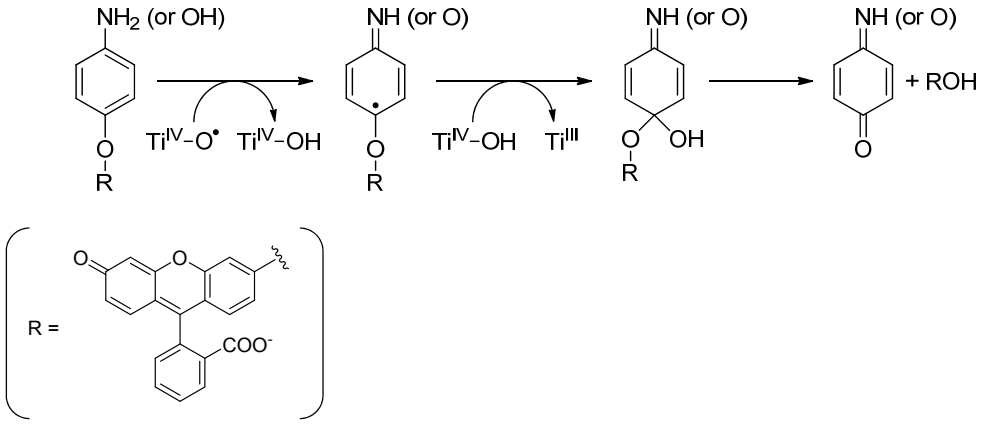

S4. Durability of CoPi-Pt-MesoTiO_2

As shown in Fig. S4, the photocatalytic activity of CoPi-Pt-MesoTiO_2 remains well after repeated use. The CoPi-Pt-MesoTiO_2 powder was collected after the reaction with APF and then washed with phosphate buffer prior to the repeated test. The slight decrease in the activity after washing might be due to the weight loss of the catalyst.

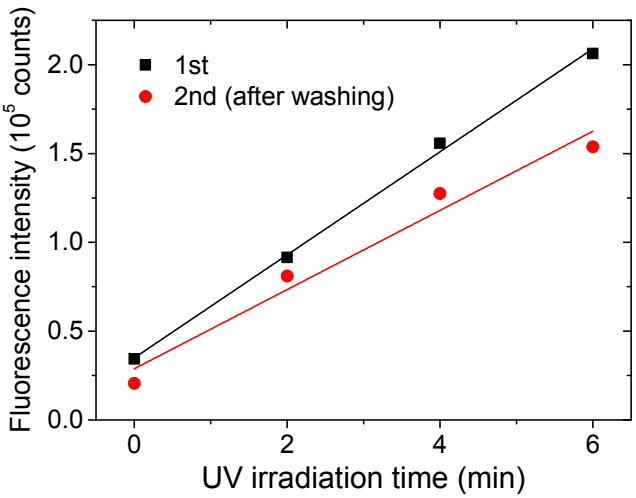

Fig. S4. UV light irradiation time dependence of fluorescence intensities of phosphate buffer suspensions containing CoPi-Pt-MesoTiO_2, APF, and DMSO.

S5. Diffusion of Fluorescent Products

The description of three-dimensional Brownian motion of a molecule in continuous medium is given as $\langle r^2 \rangle = 6Dt$, where $\langle r^2 \rangle$ is the mean-square displacement, D is the diffusion coefficient (2.8×10^{-10} m^2 s^{-1} for fluorescein[S7]), and t is the time. As demonstrated in Fig. S5, the observed rise times (t^{obs}) show linear correlation with calculated t (t^{calc}) (corrected $R^2 = 0.99$). The intercept is determined to be 17 ms, which is much longer than the photon binning time (5 ms) or the shutter opening time for UV light irradiation (0.7 ms). Considering the fact that the pore size distribution of MesoTiO$_2$ is broad (5.1 ± 2.5 nm),[S1] it is expected that the diffusion of the product fluorescein molecules (hydrodynamic radius is 0.8 nm[S8]) is partially restricted.

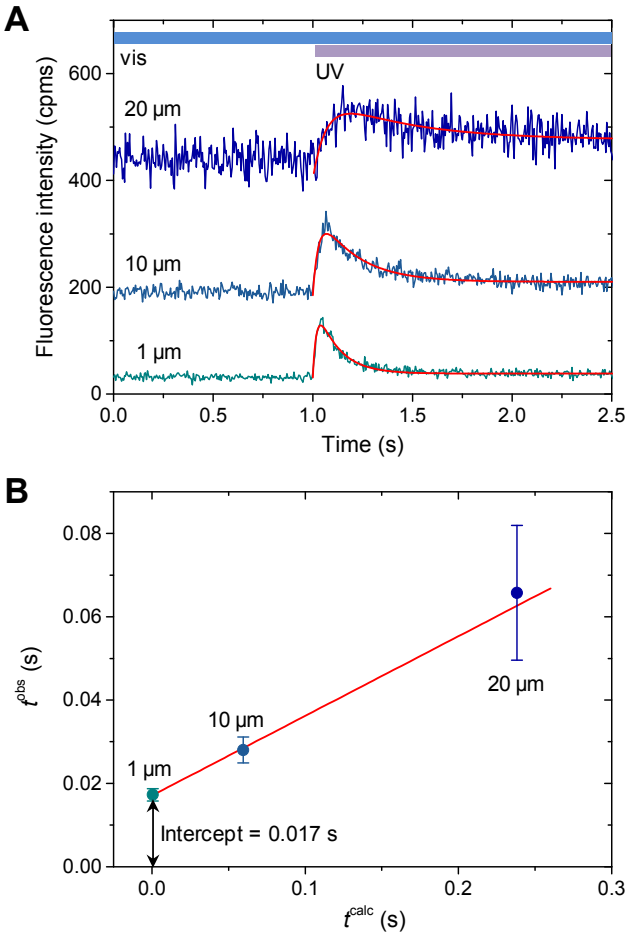

Fig. S5. (A) Time traces of fluorescence intensity measured in solution at 1, 10, and 20 μm distance from the surface of CoPi-MesoTiO$_2$ crystal. The red lines indicate the exponential growth and decay. (B) The relationship between t^{obs} and t^{calc}. The t^{obs} values were obtained as growth times by exponential fitting (see the panel A). The t^{calc} values were estimated from the equation of Brownian motion in three dimensions. See text for details.

References

S1 Z. Bian, T. Tachikawa and T. Majima, *J. Phys. Chem. Lett.*, 2012, **3**, 1422−1427.

S2 Z. Bian, T. Tachikawa, W. Kim, W. Choi and T. Majima, *J. Phys. Chem. C*, 2012, **116**, 25444−25453.

S3 K. Setsukinai, Y. Urano, K. Kakinuma, H. J. Majima and T. Nagano, *J. Biol. Chem.*, 2003, **278**, 3170−3175.

S4 G. Albarran, W. Boggess, V. Rassolov and R. H. Schuler, *J. Phys. Chem. A*, 2010, **114**, 7470–7478.

S5 T. Ohe, T. Mashino and M. Hirobe, *Tetrahedron Lett.*, 1995, **42**, 7681–7684.

S6 Y. Urano, T. Higuchi and M. Hirobe, *J, Chem. Soc. Perkin Trans. 2*, 1996, 1169–1173.

S7 K. Chattopadhyay, S. Saffarian, E. L. Elson and C. Frieden, *Proc. Natl. Acad. Sci. U. S. A.*, 2002, **99**, 14171–14176.

S8 D. S. Banks and C. Fradin, *Biophys. J.*, 2005, **89**, 2960–2971.